

Understanding the unexpected suppression patterns at RHIC and LHC

Magdalena Djordjevic

Institute of Physics Belgrade, University of Belgrade, Pregrevica 118, 11080 Belgrade, Serbia
magda@ipb.ac.rs

Marko Djordjevic

Faculty of Biology, University of Belgrade, Studentski trg 3, 11000 Belgrade, Serbia

Received 16 July 2014

Accepted 21 August 2014

Published 8 October 2014

Understanding properties of QCD matter created in ultra-relativistic heavy-ion collisions is a major goal of RHIC and LHC experiments. Suppression of light and heavy flavor observables is a powerful tool to understand these properties and the suppressions of underlying partons appear to suggest a clear hierarchy in the suppression of these observables. However, the measurements show significant qualitative differences between the observed and intuitively expected patterns, in particular for neutral pions and single electrons at RHIC and for charged hadrons and D mesons at LHC, which are denoted as heavy flavor puzzles at RHIC and LHC. In this review, we discuss these puzzles and also summarize evidence that they can be consistently explained within the same theoretical framework.

PACS Nos.: 12.38.Mh, 24.85.+p, 25.75.-q

1. Introduction

QCD predicts that, at extremely high energy densities, a new form of matter will be created.^{1,2} This form of matter, consists of interacting quarks, antiquarks and gluons, which are no longer confined. Such form of matter is called Quark–Gluon Plasma (QGP) and it is believed that it existed immediately after the Big Bang.³ Alternatively, this form of matter can be reached by experiments involving relativistic heavy-ion collisions, where heavy ions with extremely high kinetic energies are collided. Therefore, creating QGP in a lab can enable us to both learn about the properties of this fundamentally new form of matter and to study the origin of matter at its most basic level.

Therefore, one of the most important goals of high energy heavy-ion physics is to form, observe and understand QGP. With this purpose in mind RHIC (Relativistic Heavy Ion Collider) was designed at Brookhaven National Laboratory. Also, a major

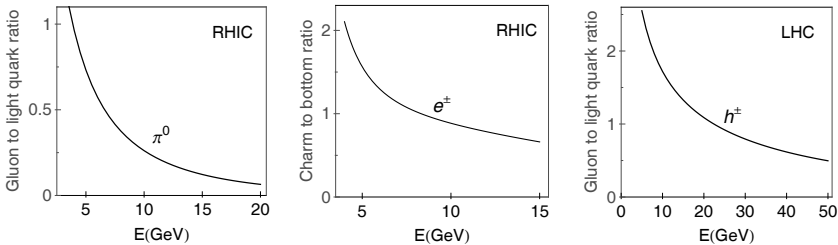


Fig. 1. Parton contribution in light hadron and single electron production at RHIC and LHC. The left panel shows the gluon to light quark contribution ratio in the initial distributions of neutral pions at RHIC. The central panel shows charm to bottom quark ratio in the initial distributions of non-photonic single electrons at RHIC. The right panel shows gluon to light quark contribution ratio in the initial distributions of charged hadrons at LHC. Panels adapted from Refs. 6 and 7.

goal of LHC (Large Hadron Collider) at CERN is to study the properties of QGP. A powerful way to analyze these properties is suppression⁴ of jets (high energy probes) that are created within the medium.

The basic idea behind the jet suppression measurements is that jets created inside the medium will lose some amount of energy due to interaction with the medium constituents.⁵ Therefore, the energy distribution of the jets leaving the medium will be suppressed compared to the energy distribution when the medium is absent. Since suppression depends on both the type of the particle and the type of the medium, detailed study (both theoretical and experimental) of the suppression patterns can enable us to learn about the properties of the matter created at RHIC and LHC.

2. The Unexpected Suppression Patterns

Suppression of light and heavy flavor observables present, in general, a powerful tool for studying the properties of QCD matter created at ultra-relativistic heavy-ion collisions. Within this, measurements of unexpected suppression hierarchies are of particular value, since theoretically addressing such observations test our quantitative and qualitative understanding of nuclear matter at extreme conditions. Such unexpected suppression hierarchies are provided by neutral pions and single electrons at RHIC, and by charged hadrons and D mesons at LHC, which we further discuss below.

From Fig. 1, one can see that for neutral pions at RHIC and charged hadrons at LHC, both light quarks and gluons significantly contribute to their production. The same figure shows that both charm and bottom contribute to non-photonic single electron production at RHIC. On the other hand, D mesons present a clear charm quark probe, since the feeddown from B mesons is subtracted from experimental data.⁸ Consequently, to further discuss the suppression patterns of the relevant observables (light hadrons, D mesons and single electrons), in Fig. 2, we show the suppression patterns of the underlying partons at both RHIC and LHC. From the

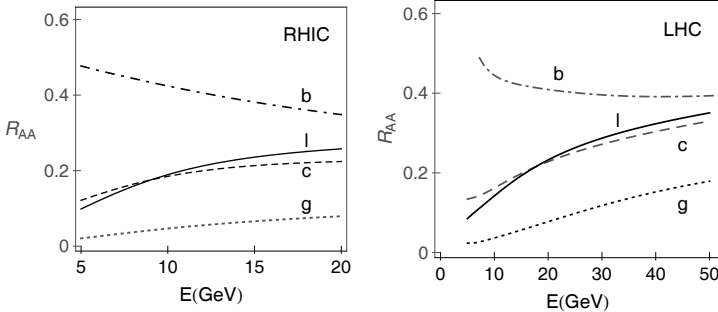


Fig. 2. Parton suppressions at RHIC and LHC. Momentum dependence of the jet suppression is shown for charm quarks (dashed curves), bottom quark (dot-dashed curves), light quarks (full curves) and gluons (dotted curves). The left panel corresponds to RHIC conditions and the right panel to LHC conditions. On each panel, electric to magnetic mass ratio is fixed to 0.4. Panels adapted from Refs. 6 and 7.

figure, we see that charm and light quark suppressions are similar, with somewhat larger charm quark suppression due to steeper initial distribution of charm quarks. Furthermore, we see that the suppression of light and charm quarks is in-between the smaller bottom suppression and the larger gluon suppression; this is due to a larger color factor for gluons and a larger mass (and consequently significant dead-cone effect) for bottom quarks. These parton suppressions then lead to the evident expectations for the suppression hierarchies of the relevant observables: (i) at RHIC, D mesons should have notably smaller suppression compared to pions, but significantly larger suppression compared to non-photonic single electrons — therefore, the measured pion suppression at RHIC should be much larger compared to the non-photonic single electron suppression, (ii) at LHC, measured D meson suppression should be notably smaller than charged hadron suppression.

However, these expectations are clearly not supported by the measured experimental data at RHIC and LHC: the left panel of Fig. 3 shows that measured suppressions for neutral pions^{9,10} and single electrons^{11,12} at RHIC are similar. This surprising observation has been called the heavy flavor puzzle at RHIC,¹³ which has up-to-now inspired a significant amount of theoretical work,¹⁴ including suggestions that the puzzle requires explanations outside conventional pQCD.^{15–18} Similar surprising experimental results are obtained for LHC, where in the right panel of Fig. 3 we see the same suppression for charged hadrons¹⁹ and D mesons.⁸ Through analogy with RHIC, this unexpected measurement was termed “heavy flavor puzzle at LHC”.⁶

It is clear that, in order to understand these surprising measurements (the heavy flavor puzzles at RHIC and LHC), it is necessary to analyze them within the same theoretical framework, and with a consistent parameter set. Regarding the parameters, it is also desirable to use no free parameters in comparing theoretical predictions with experimental data, so that parameters are fixed to standard literature values. Finally, we also argue that, to fully understand the two puzzles, one should

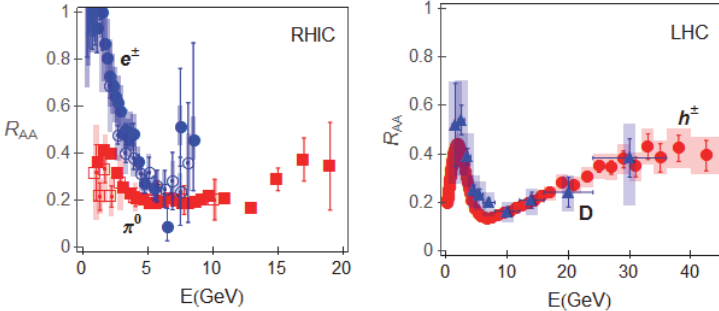


Fig. 3. (color online) Heavy flavor puzzles at RHIC and LHC. The left panel shows together the experimentally measured 0–10% central 200 GeV RHIC R_{AA} data for neutral pions (open red squares from STAR⁹ and full red squares from PHENIX¹⁰) and non-photonic single electrons (open blue circles from STAR¹¹ and full blue circles from PHENIX¹²). The right panel shows together the experimentally measured 0–5% central 2.76 Pb+Pb ALICE preliminary R_{AA} data for charged hadrons¹⁹ (the red circles) and D mesons⁸ (the blue triangles). Panels adapted from Refs. 6 and 7.

obtain not only a quantitative agreement with the measured data, but also a qualitative understanding of the underlying effects. With these, and other goals in mind, we developed the dynamical energy loss formalism for jet suppression at RHIC and LHC, which we review in the next section.

3. The Dynamical Energy Loss Formalism

We here briefly review the main ingredients of the dynamical jet energy loss formalism. The calculations follow a general scheme that involves different steps in jet propagation, which are shown in Fig. 4. As can be seen, these steps involve jet production, energy loss, fragmentation and decay (in the case of heavy mesons), so reliable calculations of these steps are important. It is widely considered that jet energy loss is the critical step in the suppression calculations, so we first review this step below. We will however, see that, contrary to the widely held belief, jet fragmentation and decay also play a crucial role in explaining the puzzles at RHIC and LHC, so we will below also discuss other steps in the computational procedure:

(i) *Dynamical scattering centers:* Most of the previous energy loss calculations were based on the assumption of static scattering centers.²⁰ However, this

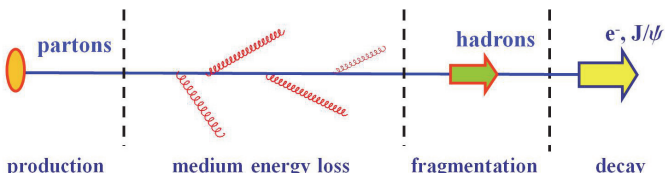


Fig. 4. Jet propagation scheme. The scheme illustrates different steps which are involved in jet propagation, emphasizing that the calculations separately (and consecutively) treat jet production, medium energy loss, fragmentation and decay.

assumption is inherently inconsistent, since energy loss calculations show that radiative and collisional energy losses are comparable,^{21–23} but the static medium approximation necessarily leads to zero collisional energy loss.²⁴ Therefore, QCD medium cannot be realistically modeled by static scattering centers and dynamical effect of medium partons has to be taken into account in jet energy loss calculations.

We consequently developed the jet energy loss formalism, which calculates collisional²³ and radiative energy loss,^{24,25} in a finite size dynamical QCD medium. The formalism takes into account that the scattering centers are in reality dynamical (i.e. moving) particles, where the calculations are implemented in a medium of realistic (finite) size; the calculations were employed by using hard-thermal-loop approach. Also, it is important to note that both electric and magnetic contributions now appear in the energy loss results,²⁶ which is in distinction to the static case where only the electric contribution appears. The appearance of the magnetic contribution in the energy loss, then leads to a question of how finite magnetic mass could influence this energy loss result, which we next address.

(ii) *Finite magnetic mass*: While pQCD calculations assume zero magnetic mass, different nonperturbative approaches suggest a nonzero magnetic mass at RHIC and LHC.^{27–30} This therefore raises an important question of consistently including finite magnetic mass in energy loss calculations. We consequently generalized the dynamical energy loss formalism to the case of finite magnetic mass³¹ by using generalized sum-rules. Briefly, the calculation of the energy loss can be separated in two parts: in the first part, which corresponds to jet interaction with the medium, the finite magnetic mass can be introduced through the generalized sum-rules. The second part, which corresponds to gluon radiation, is purely perturbative, and is not modified by introducing the magnetic screening.

(iii) *Running coupling*: We factorized the coupling to the part that corresponds to the interaction between the jet and the radiated gluon and the part that corresponds to the interaction of the jet with the exchanged gluon (details of the procedure are presented in Ref. 32). Note that the introduced running coupling is infrared safe, so that there is no need to employ the artificial cutoffs, as is commonly done in other studies.^{33,34}

(iv) *The suppression calculation procedure*: We furthermore integrated the dynamical energy loss into an up-to-date numerical procedure for the suppression predictions.³² The procedure takes into account multigluon³⁵ and path-length^{36,37} fluctuations, and most up-to-date functions for jet production,^{38,39} fragmentation for light⁴⁰ and heavy flavor,^{41,42} and, in the case of heavy mesons, their decay to single electrons.³⁸ For the temperature, for LHC we used effective temperature of 304 MeV, as extracted by ALICE,⁴³ while for RHIC, we used effective temperature of 225 MeV, as extracted by PHENIX.⁴⁴ The details of the numerical procedure, as well as the rest of the parameters are specified in Ref. 32. Note that we use no free parameters, i.e. all the parameters used in our calculations correspond to standard literature values.

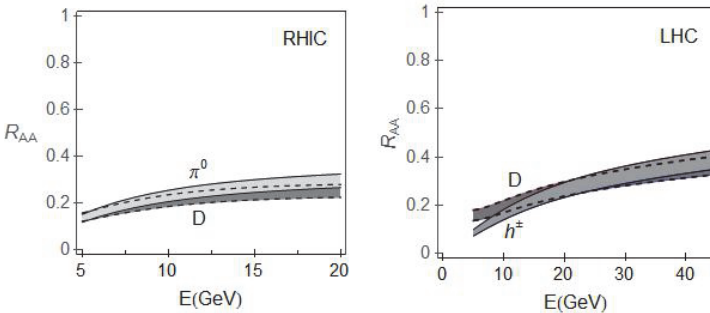


Fig. 5. Comparison of pion and D meson suppression predictions at RHIC and LHC. The left panel shows the comparison of neutral pion suppression predictions (light gray band) with D meson (dark gray band) suppression predictions, as a function of momentum, for RHIC case. The right panel shows the comparison of charged hadron suppression predictions (light gray band) with D meson (dark gray band) suppression predictions, as a function of momentum, for LHC case. On each panel gray regions correspond to $0.4 < \mu_M / \mu_E < 0.6$,^{27–30} where the upper (lower) boundary on each band corresponds to $\mu_M / \mu_E = 0.6$ ($\mu_M / \mu_E = 0.4$). Panels adapted from Refs. 6 and 7.

In summary, to analyze the puzzling experimental data, we developed a framework that takes into account both collisional and radiative energy loss in a dynamical, finite size, QCD medium. This approach both takes into account that the scattering centers are in reality dynamical and includes finite magnetic mass and running coupling. Consequently, this framework employs a complete jet energy loss formalism, which addresses both light and heavy flavor observables in a finite size optically thin QCD medium. In the following sections, we will employ this formalism to quantitatively and qualitatively analyze the heavy flavor puzzles at RHIC and LHC.

4. The Effects Behind the Puzzle

We will here summarize the evidence that the essence of both the puzzles (at RHIC and LHC) is a surprising reversal of hierarchy between D mesons and light hadrons. With respect to this, note that the suppression patterns of the underlying partons lead to an intuitive expectation that the light hadron suppression should be notably larger compared to D meson suppression (see Fig. 2 and the corresponding discussion); as discussed above, this is clearly not supported by the data. Even more surprisingly, the expected hierarchy is also not supported by our theoretical predictions, which are generated by the computational framework described in the previous section. In Fig. 5, we see that for both RHIC and LHC the predicted light hadron suppression is the same or even smaller compared to the predicted D meson suppression. Below we aim to understand the effects behind these surprising measurements.

Our assumption was that fragmentation functions can play a major role^{6,7} in the unexpected predictions shown in Fig. 5; this is because these functions are

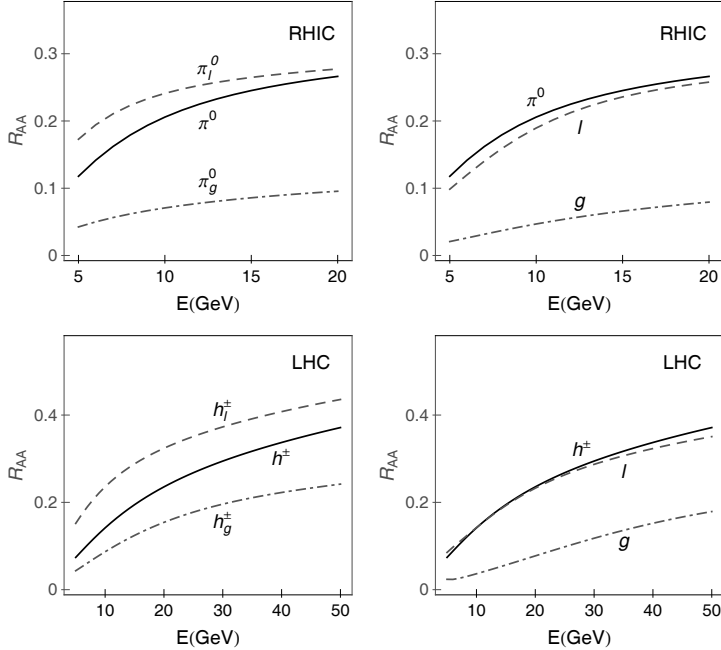


Fig. 6. Comparison of the light flavor suppression predictions at RHIC (upper panels) and LHC (lower panels). In the upper left panel, the dashed curve shows what would be the neutral pion suppression if only light quarks would contribute to pions. The dot-dashed curve shows what would be the neutral pion suppression if only gluons would contribute to pions, while the full curve shows the actual neutral pion suppression predictions. The upper right panel shows the comparison of neutral pion suppression predictions (full curve) with light quark (the dashed curve) and gluon (the dot-dashed curve) suppression predictions, as a function of momentum. In the lower left panel, the dashed curve shows what would be the charged hadron suppression if only light quarks would contribute to hadrons. The dot-dashed curve shows what would be the charged hadron suppression if only gluons would contribute to hadrons, while the full curve shows the actual charged hadron suppression predictions. The lower right panel shows the comparison of charged hadron suppression predictions (full curve) with light quark (the dashed curve) and gluon (the dot-dashed curve) suppression predictions, as a function of momentum. On each panel, electric to magnetic mass ratio is fixed to $\mu_M/\mu_E = 0.4$. Panels adapted from Refs. 6 and 7.

responsible for the transfer from the parton to the hadron level. First, one should note that charm and bottom suppressions are not modified by D and B meson fragmentation functions,^{6,7} so that suppressions of D and B mesons indeed genuinely reflect those of charm and bottom quarks. On the other hand, there is a much more complex interplay between the suppression and fragmentation for light hadrons,^{6,7} which we further investigate below.

The upper left panel of Fig. 6 shows what would be pion suppression if pions were composed only of light quarks (the dashed curve), or of only gluons (the dot-dashed curve). We see that, as expected, the pion suppression is in-between the two curves. On the other hand, the upper right panel of the same figure, shows the comparison of the pion suppression with the bare light quark and gluon suppressions;

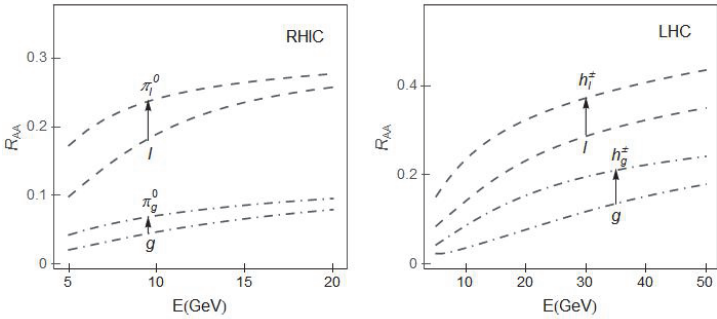


Fig. 7. Modifying the suppression patterns by the fragmentation functions. The left panel shows the comparison of neutral pion suppression at RHIC if only light quarks would contribute to pions (upper dashed curve) with bare light quark suppression (lower dashed curve), as well as the comparison of neutral pion suppression if only gluons would contribute to pions (upper dot-dashed curve) with bare gluon suppression (lower dot-dashed curve). The right panel shows the comparison of charged hadron suppression at LHC if only light quarks would contribute to charged hadrons (upper dashed curve) with bare light quark suppression (lower dashed curve), as well as the comparison of charged hadron suppression if only gluons would contribute to charged hadrons (upper dot-dashed curve) with bare gluon suppression (lower dot-dashed curve). The arrows indicate the suppression decrease due to fragmentation functions.

surprisingly, we see that the pion suppression is lower than even the bare light quarks suppression. This surprising result can be understood if one compares the dashed (and the dot-dashed) curves in the upper left and the upper right panels of Fig. 6. For more clarity, these curves are presented together and compared in the left panel of Fig. 7. From this panel, we see that the fragmentation functions modify the suppression curves, so that the fragmentation substantially lowers the bare light quark and gluon suppressions. This significant decrease in the suppression due to the fragmentation then explains the unintuitive suppression hierarchy that can be observed when comparing the pion suppressions with the bare light quark and gluon suppressions (the upper right panel of Fig. 6). This unintuitive hierarchy, i.e. the fact that pions have a smaller suppression than bare light quarks together with the fact that charm suppression is somewhat larger than bare light quark suppression, and that charm quarks are genuine probes of D mesons suppression, directly lead to the surprising result of larger pion compared to D meson suppression⁷ (the left panel in Fig. 5).

Similarly, the deformation of the suppression patterns by the fragmentation functions is also a major cause behind the surprising — both measured and predicted — result that the charged hadron suppression has the same value as D meson suppression at LHC; evidence for this is provided in the two lower panels in Fig. 6. In the lower left panel, we see what would be the charged hadron suppression if charged hadrons were composed only of light quarks (the dashed curve) or only of gluons (the dot-dashed curve). These two curves are compared with the actual hadron suppression (the full curve) that is — as expected — in between the two curves. On the other hand, in the lower right panel, we see that the hadron

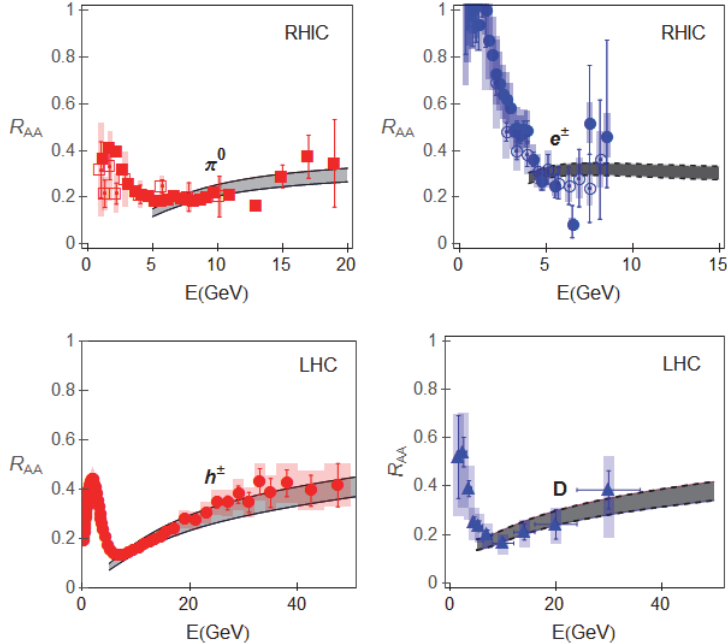


Fig. 8. (color online) Comparison of light and heavy flavor suppression predictions with experimental data. The upper left panel compares theoretical predictions for neutral pion suppression (light gray band) with available pion R_{AA} data at 0–10% central 200 GeV collisions at RHIC (open red squares from STAR⁹ and full red squares from PHENIX¹⁰). The upper right panel compares theoretical predictions for single electron suppression with non-photonic single electron R_{AA} data at 0–10% central 200 GeV collisions at RHIC (open blue circles from STAR¹¹ and full blue circles from PHENIX¹²). The lower left panel shows the comparison of charged hadron suppression predictions with experimentally measured R_{AA} data (red circles) for charged particles from ALICE¹⁹ 0–5% central 2.76 TeV Pb+Pb collisions at LHC. The lower right panel shows the comparison of D meson suppression predictions with D meson R_{AA} (blue triangles) from ALICE⁸ 0–7.5% central 2.76 TeV Pb+Pb collisions at LHC. Gray regions correspond to $0.4 < \mu_M/\mu_E < 0.6$, where the upper (lower) boundary on each band corresponds to $\mu_M/\mu_E = 0.6$ ($\mu_M/\mu_E = 0.4$). Panels adapted from Refs. 6 and 7.

suppression, unexpectedly, overlaps the bare light quark suppression. Similarly as with RHIC, the reason behind the unexpected result is a substantial lowering of the bare light quark and gluon suppressions due to fragmentation, which can be directly observed in the right panel of Fig. 7. Therefore, the lower right panel in Fig. 6, together with Fig. 2, and the fact that D meson is a genuine charm quark probe, clearly explains the experimental result that charged hadron suppression is approximately the same as D meson suppression (for more details see Ref. 6).

5. Explaining the Puzzles

The results in the previous section that charged hadron and pion suppressions are similar (and even somewhat smaller in the pion case) to the D meson suppression, provide qualitative explanation for the heavy flavor puzzles at RHIC and LHC. In

the case of LHC, the theoretical result that charged hadron suppression is almost the same as D meson suppression directly explains the measured data, and consequently provides the qualitative explanation of the heavy flavor puzzle at LHC. For RHIC experiments, one should note that the decay functions modify D and B meson suppression patterns, so that single electron suppression approaches D meson suppression (for more details see Ref. 7). This result, together with the obtained somewhat smaller suppression of pions relative to D mesons, then provides a clear qualitative explanation of the heavy flavor puzzle at RHIC, i.e. of the surprising experimental observation that single electron suppression approaches neutral pion suppression.

In addition to the qualitative explanation, we also want to test if we can obtain an accurate quantitative description for heavy flavor puzzles at RHIC and LHC. In the upper left and right panels of Fig. 8, we compare, respectively, the predicted neutral pion and single electron suppressions, with the experimentally measured data. We here observe an excellent agreement of the theory with the experimental measurements, which is achieved with no free parameters in the comparison (i.e. all the parameters are fixed to standard literature values). Similarly, in the two lower panels of the same figure, we see that the theoretical predictions can equally well explain the suppressions of pions and D mesons at LHC. We consequently conclude that the theory is able to provide both qualitative and quantitative explanations of the heavy flavor puzzles at RHIC and LHC.

6. Conclusions

The suppression measurements at RHIC and LHC reveal intuitively surprising suppression hierarchies. These observations at RHIC, which inspired a significant amount of theoretical work in the past, were called “the heavy flavor puzzle at RHIC”, while the equivalent surprising measurements at LHC were termed “the heavy flavor puzzle at LHC”. Theoretically explaining these measurements provides opportunity to test not only if our current understanding of the nuclear matter at extreme conditions can quantitatively explain the data, but also if we can generate nontrivial qualitative understanding of the effects behind the puzzles. To generate such understandings, we employed a state of the art energy loss formalism, whose main ingredient is a dynamical description of the scattering centers in a realistic finite size, optically thin, QCD medium. We here reviewed evidence that this framework, under the same assumptions, and with no free parameters in comparison with experimental data, can jointly explain both puzzles at RHIC and LHC. Even more importantly, we were able to trace the qualitative effects that are behind the two puzzles. It turns out that the essence of both puzzles is an unexpected reversal of the suppression hierarchy between light hadrons and D mesons. This reversal of the hierarchy is a consequence of a complex interplay of energy loss and fragmentation patterns, where a major effect is a substantial lowering of bare light quark and gluon suppressions due to fragmentation.

In summary, the ability of theory to explain such puzzling data strongly argues that pQCD can provide an accurate description of the nuclear matter created in ultra-relativistic heavy-ion collisions. In an outlook, such agreement, together with other recent analysis,^{32,45} also strongly suggest that a single theory, within the same theoretical framework, can explain a wide range of probes under different experimental conditions, possibly also outside of the energy ranges explored in this review. We believe that achieving this will require not only systematic comparisons of the theoretical predictions with experimental data, but also substantial future improvements in the theoretical formalism.

Acknowledgments

This work is supported by Marie Curie International Reintegration Grant within the 7th European Community Framework Programme (PIRG08-GA-2010-276913) and by the Ministry of Science and Technological Development of the Republic of Serbia, under projects Nos. ON171004 and ON173052.

References

1. J. C. Collins and M. J. Perry, *Phys. Rev. Lett.* **34**, 1353 (1975).
2. G. Baym and S. A. Chin, *Phys. Lett. B* **62**, 241 (1976).
3. R. Stock, *Nature* **337**, 319 (1989).
4. J. D. Bjorken, FERMILAB-PUB-82-059-THY (1982) 287, 292.
5. M. Gyulassy, *Lect. Notes Phys.* **583**, 37 (2002); X. N. Wang and M. Gyulassy, *Phys. Rev. Lett.* **68**, 1480 (1992).
6. M. Djordjevic and M. Djordjevic, *Phys. Rev. Lett.* **112**, 042302 (2014).
7. M. Djordjevic and M. Djordjevic, *Phys. Rev. C* **90**, 034910 (2014).
8. A. Grelli (for the ALICE Collab.), *Nucl. Phys. A* **904-905**, 635c (2013).
9. STAR Collab. (B.I. Abelev *et al.*), *Phys. Rev. C* **80**, 44905 (2009).
10. PHENIX Collab. (A. Adare *et al.*), *Phys. Rev. Lett.* **101**, 232301 (2008).
11. STAR Collab. (B. I. Abelev *et al.*), *Phys. Rev. Lett.* **98**, 192301 (2007).
12. PHENIX Collab. (A. Adare *et al.*), *Phys. Rev. Lett.* **98**, 172301 (2007).
13. M. Djordjevic, *J. Phys. G* **32**, S333 (2006).
14. M. Gyulassy, *Physics* **2**, 107 (2009).
15. A. Ficnar, J. Noronha and M. Gyulassy, arXiv:1106.6303.
16. J. Noronha, M. Gyulassy and G. Torrieri, arXiv:0906.4099.
17. S. S. Gubser *et al.*, *JHEP* **0810**, 052 (2008); P. M. Chesler *et al.*, *Phys. Rev. D* **79**, 125015 (2009).
18. W. A. Horowitz and M. Gyulassy, *Phys. Lett. B* **666**, 320 (2008); B. Betz *et al.*, *ibid.* **675**, 340 (2009).
19. ALICE Collab. (K. Aamodt *et al.*), *Phys. Lett. B* **720**, 52 (2013).
20. M. Gyulassy and X. N. Wang, *Nucl. Phys. B* **420**, 583 (1994); X. N. Wang, M. Gyulassy and M. Plumer, *Phys. Rev. D* **51**, 3436 (1995).
21. M. G. Mustafa, *Phys. Rev. C* **72**, 014905 (2005); M. G. Mustafa and M. H. Thoma, *Acta Phys. Hung. A* **22**, 93 (2005).
22. A. K. Dutt-Mazumder, Jan-e Alam, P. Roy and B. Sinha, *Phys. Rev. D* **71**, 094016 (2005).
23. M. Djordjevic, *Phys. Rev. C* **74**, 064907 (2006).

24. M. Djordjevic and U. Heinz, *Phys. Rev. Lett.* **101**, 022302 (2008).
25. M. Djordjevic, *Phys. Rev. C* **80**, 064909 (2009).
26. M. Djordjevic, *J. Phys. G* **39**, 045007 (2012).
27. WHOT-QCD Collab. (Yu. Maezawa *et al.*), *Phys. Rev. D* **81** 091501 (2010); *ibid., PoS Lattice* 194 (2008).
28. A. Nakamura, T. Saito and S. Sakai, *Phys. Rev. D* **69**, 014506 (2004).
29. A. Hart, M. Laine and O. Philipsen, *Nucl. Phys. B* **586**, 443 (2000).
30. D. Bak, A. Karch and L. G. Yaffe, *JHEP* **0708**, 049 (2007).
31. M. Djordjevic and M. Djordjevic, *Phys. Lett. B* **709**, 229 (2012).
32. M. Djordjevic and M. Djordjevic, *Phys. Lett. B* **734**, 286 (2014).
33. B. G. Zakharov, *JETP Lett.* **88**, 781 (2008).
34. A. Buzzatti and M. Gyulassy, *Nucl. Phys. A* **904-905**, 779c (2013).
35. M. Gyulassy, P. Levai and I. Vitev, *Phys. Lett. B* **538**, 282 (2002).
36. S. Wicks, W. Horowitz, M. Djordjevic and M. Gyulassy, *Nucl. Phys. A* **784**, 426 (2007).
37. A. Dainese, *Eur. Phys. J. C* **33**, 495 (2004).
38. M. Cacciari, S. Frixione, N. Houdeau, M. L. Mangano, P. Nason and G. Ridolfi, *JHEP* **1210**, 137 (2012).
39. Z. B. Kang, I. Vitev and H. Xing, *Phys. Lett. B* **718**, 482 (2012); R. Sharma, I. Vitev and B. W. Zhang, *Phys. Rev. C* **80**, 054902 (2009).
40. D. de Florian, R. Sassot and M. Stratmann, *Phys. Rev. D* **75**, 114010 (2007).
41. M. Cacciari and P. Nason, *JHEP* **0309** 006 (2003); E. Braaten, K.-M. Cheung, S. Fleming and T. C. Yuan, *Phys. Rev. D* **51**, 4819 (1995).
42. V. G. Kartvelishvili, A. K. Likhoded and V. A. Petrov, *Phys. Lett. B* **78**, 615 (1978).
43. M. Wilde (for the ALICE Collab.), *Nucl. Phys. A* **904-905**, 573c (2013).
44. A. Adare *et al.*, *Phys. Rev. Lett.* **104**, 132301 (2010).
45. M. Djordjevic, M. Djordjevic and B. Blagojevic, *Phys. Lett. B* **737**, 298 (2014).